

Elastic Scattering Susceptibility of the High Temperature Superconductor $\text{Bi}_2\text{Sr}_2\text{CaCu}_2\text{O}_{8+\delta}$: A Comparison between Real and Momentum Space Photoemission Spectroscopies

K. McElroy,¹ G.-H. Gweon,² S. Y. Zhou,² J. Graf,¹ S. Uchida,³ H. Eisaki,⁴ H. Takagi,^{5,6,7} T. Sasagawa,^{5,6} D.-H. Lee,^{1,2} and A. Lanzara^{1,2}

¹*Material Sciences Division, Lawrence Berkeley National Lab., Berkeley, CA 94720 USA**

²*Physics Department, University of California Berkeley, CA 94720 USA*

³*Department of Physics, University of Tokyo, Yayoi, 2-11-16 Bunkyo-ku, Tokyo 113-8656, Japan*

⁴*AIST, 1-1-1 Central 2, Umezono, Tsukuba, Ibaraki, 305-8568 Japan.*

⁵*Department of Advanced Materials Science, University of Tokyo, Kashiwa, Chiba 277-8561, Japan*

⁶*CREST, Japan Science and Technology Agency, Saitama 332-0012, Japan*

⁷*RIKEN (The Institute of Physical and Chemical Research), Wako 351-0198, Japan*

(Dated: November 5, 2018)

The joint density of states (JDOS) of $\text{Bi}_2\text{Sr}_2\text{CaCu}_2\text{O}_{8+\delta}$ is calculated by evaluating the autocorrelation of the single particle spectral function $A(\vec{k}, \omega)$ measured from angle resolved photoemission spectroscopy (ARPES). These results are compared with Fourier transformed (FT) conductance modulations measured by scanning tunneling microscopy (STM). Good agreement between the two experimental probes is found for two different doping values examined. In addition, by comparing the FT-STM results to the autocorrelated ARPES spectra with different photon polarization, new insight on the form of the STM matrix elements is obtained. This shines new light on unsolved mysteries in the tunneling data.

Atomically resolved spectroscopic studies taken by scanning tunneling microscopy (STM) have given great insights into the low energy electronic structure of high T_c superconductors. In particular, recent work using Fourier transform STM (FT-STM) to study modulations in the local density of states (LDOS)[1, 2, 3, 4, 5] have generated a great deal of interest[6, 7, 8, 9]. When these modulations are analyzed within a simple quasi-particle interference model, motivated by the joint density of states (JDOS)[6], a bridge between the momentum space probe angle resolved photoemission spectroscopy (ARPES) and the real space probe STM has been established.[3, 4, 5] This connection proves that STM and ARPES are consistent measurements of the same underlying physical phenomenon. In addition, it allows for the two diametrically opposite spectroscopic probes to compliment each other.

Recently, R. Markiewicz [10] proposed a way to check the validity of the JDOS model by comparing the FT-STM result to the autocorrelation between the ARPES spectra (AC-ARPES). In this Letter we report on such an analysis. In addition to providing additional support to the JDOS picture[1, 3, 6], we find that the autocorrelated ARPES spectra undergoes significant variation as the photon polarization is changed. We propose that by comparing them with the FT-STM result, we learn valuable information about the STM matrix element. If our proposal is correct, some of the long standing puzzles in the STM data can be resolved. These include the lack of zero-bias peak in the tunneling spectra in the vortex core[11], and the saturation of the quasiparticle interference wave vectors near the Fermi energy (E_F)[3, 8].

We begin by briefly discussing what STM and ARPES

measure. First, STM measures the tunneling current between an atomically sharp tip and a clean flat surface at an energy ω , relative to the E_F , and at a location \vec{r} . Within the independent tunneling approximation differential conductance, $g(\vec{r}, \omega)$, is given by:

$$g(\vec{r}, \omega) = I_0 |M_{f,i}^{\vec{r}}|^2 R(\omega) A(\vec{r}, \omega) \quad (1)$$

where $M_{f,i}^{\vec{r}}$ is the tunneling matrix element, $R(\omega)$ is due to the finite resolution of the STM, and $A(\vec{r}, \omega)$ is the real space single particle spectral function, commonly referred to as the ‘‘LDOS’’[12]. On the other hand, ARPES measures the photo current $I(\hat{e}, \vec{k}, \omega)$ of electrons ejected from a surface by UV and x-ray photons. In the sudden approximation the photo current is given by:

$$I(\hat{e}, \vec{k}, \omega) = I_0 |M_{f,i}^{\hat{e}}|^2 f(\omega) A(\vec{k}, \omega) \quad (2)$$

where $M_{f,i}^{\hat{e}}$ are the photoemission matrix elements (which depends on, among other things, the photon polarization \hat{e}), $f(\omega)$ is the Fermi function, and $A(\vec{k}, \omega)$ is the momentum space single particle spectral function[13].

To check the JDOS picture[10] one needs to calculate the JDOS directly from ARPES measured $A(\vec{k}, \omega)$ by taking the following autocorrelation

$$\text{JDOS}(\vec{q}, \omega) = \int A(\vec{k} + \vec{q}, \omega) A(\vec{k}, \omega) d^2k. \quad (3)$$

Thus, barring matrix element effects (which we will come back to), the AC-ARPES gives the susceptibility of a system to scattering within the JDOS model.

Here we report such a AC-ARPES study on the high temperature superconductor $\text{Bi}_2\text{Sr}_2\text{CaCu}_2\text{O}_{8+\delta}$ for

two different doping values in the superconducting regime[14]. When compared, the AC-ARPES results and the corresponding FT-STM data show good agreement for energy smaller than the superconducting gap. At higher energies, additional weak features along the (π, π) direction, not reported by FT-STM, are observed. Most importantly by changing the photon polarization from the nodal (Γ -X) to the antinodal (Γ -M)) direction we suppress the contribution from the nodal quasiparticles in the AC-ARPES. Interestingly, when this is done, the AC-ARPES agrees better with the FT-STM data. We propose that this supports the STM matrix element having a similar suppression of the nodal states[15, 16].

The experiments were carried out at beam line 10.0.1 of the Advanced Light Source of the Lawrence Berkeley National Laboratory and beam line 5.4 of the Stanford Synchrotron Radiation Laboratory. Data from two representative $\text{Bi}_2\text{Sr}_2\text{CaCu}_2\text{O}_{8+\delta}$ samples are presented. Both samples were measured with 0.15° angular resolution in the superconducting state at 25 K. The underdoped (UD64K) sample, T_c of 64 K, was measured with polarization $\hat{e} \parallel \Gamma\text{M}$, $h\nu = 22$ eV and energy resolution of 22 meV. The optimally doped sample (OPT92K), T_c of 92 K, was measured with $\hat{e} \parallel \Gamma\text{X}$, $h\nu = 33$ eV and resolution of 15 meV.

Figure 1a shows a map of the ARPES spectral intensity at E_F for the UD64K sample. Data were taken in the irreducible first Brillouin zone and symmetrized. The high intensity points (black) form typical arcs (banana shaped contours) near the nodal direction and gap of spectral intensity as we approach the antinodal point M, as expected for a d-wave superconductor. For clarity, we have used a low intensity cutoff (less than 1/3 of the maximum value) to suppress the contribution from the first and second order superstructure replicas; this cutoff has no other effect on the results discussed in this Letter. In this case an additional suppression of spectral intensity is evident along the nodal direction which is caused by the ARPES matrix element [17] associated with the incoming photon polarization, $\hat{e} \parallel \Gamma\text{M}$. In panels b)-e) we show the autocorrelated ARPES spectra[18] for several energies below E_F . The maps exhibit distinctive patterns of peaks, whose \vec{q} -vectors disperse as the binding energy increases. The qualitative features shown in Fig. 1 are robust across different dopings; however, they become less distinct in the overdoped regime.

In order to characterize these peaks, as well as compare them with the FT-STM results, we show, in Figure 2, a direct comparison between the FT-STM map (panel a)[4] and AC-ARPES map (panel b) for a similar doping and energy. All peaks in the AC-ARPES map are symmetry related to the set of circles which are labeled using the notation used in Ref.[3]. Each of the q_i are the wave vectors transfer associated with the elastic scattering between an ‘octet’ of momenta[3] (see inset in Fig. 2 panel a)). Good agreement between the two spectroscopies is

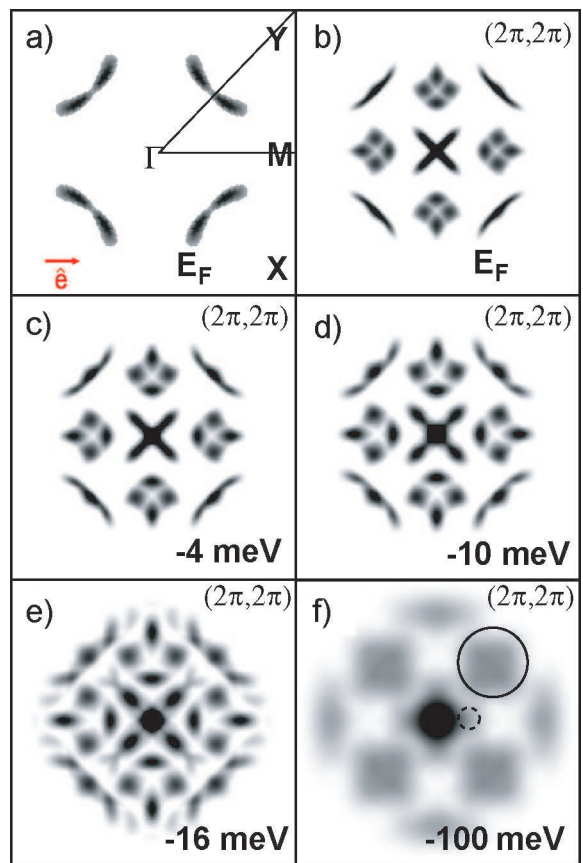


FIG. 1: a) ARPES photo current intensity measured in the octant (indicated by the triangle) and then reflected to fill in the first Brillouin zone for the UD64K sample. The red arrow shows the polarization of the incoming photons relative to the crystal structure. b)-e) Autocorrelations of the ARPES intensity at E_F , -4, -10, -16 meV respectively. 32 different peaks can be seen that disperse in a systematic fashion as a function of energy. The same color scale is used in all the panels where black represent maxima of intensity and white zero intensity. f) Autocorrelation of ARPES intensity at -100 meV (outside the superconducting gap). Weak features along $\vec{q} \parallel (\pi, \pi)$ (solid circle) can still be seen. Additionally no well defined feature at $\vec{q} \approx (0, 2\pi/4.5a_0)$ is seen at this energy (dashed circle).

observed in the sense that not only are all of the patterns present in the AC-ARPES map also observed in the FT-STM map, but they appear to occur at similar momentum locations. Additionally, even the shapes of these patterns agrees very well between the two maps. For example, the orientations of the ‘cigar’ shaped q_1 and q_5 are similar in both maps with the four q_1 ’s making a square while the four q_5 ’s make a cross. In the case of the AC-ARPES we can clearly also distinguish q_4 which is not easily identified by FT-STM [3].

This analysis can be extended to energies outside the superconducting gap energy. In particular, an additional q vector $\vec{q}^* \approx (2\pi/4.5a_0, 0)$ has been reported between binding energies of 65 and 150 meV in underdoped sam-

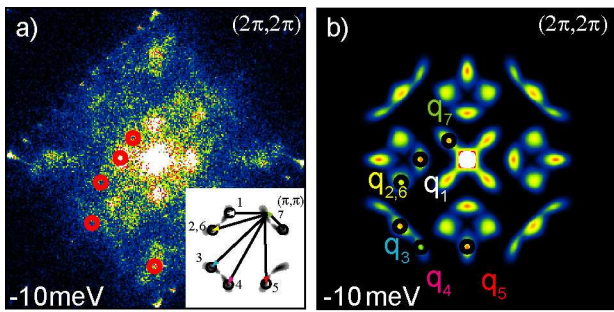


FIG. 2: a) FT-STM intensity at -10 meV adapted from [3]. Red circles mark the peaks associated with the ‘octet’ model. b) A representative AC-ARPES result at -10 meV with same peaks identified. The scattering processes and designations that result in the ‘octet’ peaks seen in these two panels are shown in the inset in panel a).

ples and interpreted as evidence of a competing charge order parameter[5]. Fig. 1 f) shows the AC-ARPES for a similar doping and energy (-100 meV). No distinct feature is visible near \vec{q}^* (dashed circle Fig. 1 f)) in the AC-ARPES analysis. The fact that \vec{q}^* does not show up in the AC-ARPES suggests that it is not a quasiparticle interference feature supporting the interpretation that it is due to enhanced scattering from a competing order parameter[5, 19]. Also, at -100 meV the AC-ARPES shows a weak, previously unreported feature along $\vec{q} \parallel (\pi, \pi)$ (solid circle) in Fig. 1 f). We believe this feature is due to the flat band located around $(\pm\pi, 0)$ and $(0, \pm\pi)$. It will be interesting if this feature is also seen by FT-STM.

To get a quantitative comparison between these results, we show in Fig. 3 cuts through the AC-ARPES data along high symmetry axes, for $q \parallel (\pi, 0)$ (panel a) and $q \parallel (\pi, \pi)$ (panel b). By following the local maxima of these peaks as a function of energy we have extracted the dispersion relation for each of the vectors. The resulting \vec{q} -vector dispersions are plotted in Fig. 3 c) and d) (filled symbols) and are compared with the FT-STM results [5] for a similar sample (open symbols).

We note here that, within a quasiparticle scattering theory, there are other, off-shell, terms that contribute to the LDOS. However, the excellent agreement between the two probes shown here suggests that equation 3 is the dominant contribution to the spatial-varying LDOS. Although this is in agreement with single-impurity T-matrix calculations[6], the physical reason is unknown.

The above successful comparison between AC-ARPES and the FT-STM suggests the validity of the JDOS picture in the quasiparticle interference model[1, 3, 5, 6]. Now we turn to a main point of this Letter - the photon polarization dependence of the agreement between the AC-ARPES and the FT-STM. Until now we have swept under the rug the fact that the ARPES intensity is not simply $A(\vec{k}, \omega)$ (Eqn. 2). Aside from the Fermi

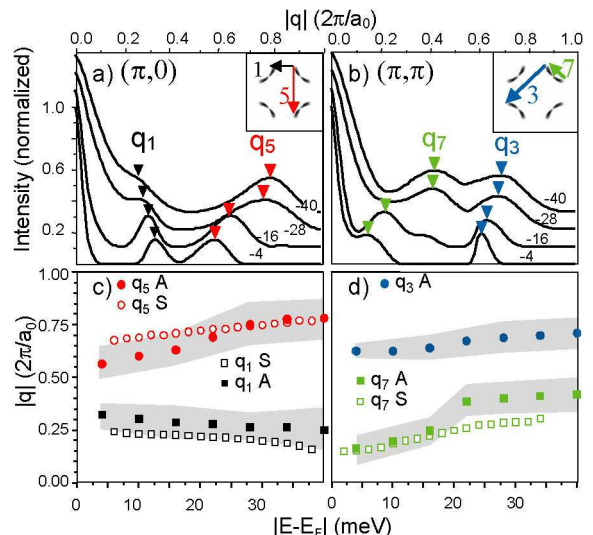


FIG. 3: a) Line cut parallel to $(\pi, 0)$ through the AC-ARPES map for several energies (-4, -16, -28, -40 meV) near the E_F , for the UD64K sample. For clarity each curve’s maximum was normalized to unity. Dispersing peaks are indicated by triangles. b) Linecut parallel to (π, π) through the AC-ARPES map for the same energies as in panel a. c-d) Peak locations from AC-ARPES (full symbols), identified with the corresponding q -vectors from the octet model, as a function of energy for peaks in the $(\pi, 0)$ (panel c) and (π, π) (panel d) direction. Corresponding STM peaks from [5] are also plotted (empty symbols) for a similar doping. The gray areas represent the FWHM of the peaks. No published FT-STM data exists for q_3 at a similar doping.

function (which has little effect at low temperature and non-zero binding energy), the ARPES spectra contain a matrix element which depends on the polarization of the incident photon. Thus far, we have used the data with photon polarization along ΓM . Such photon polarization suppresses the states in the ΓY direction[17]. In the literature a similar suppression of nodal states in the STM spectra has been suggested to exist. This has been used to explain the spatial pattern of the impurity states [15], and the lack of a zero-bias conductance peak in the vortex core[16]. Until now, however, investigating the tunneling matrix element has been limited by the lack of control that experimenters have over the tip wavefunction upon which it depends [12].

Figure 4 illustrates the effect of changing the photon polarization on our comparison. In panel 4 a) we show the AC-ARPES obtained for photons with polarization parallel to the ΓX direction (red arrow) for the 92KOPT sample. In this geometry the intensity in the FS map (see inset of Fig. 4 b) is enhanced along the nodal direction with respect to the previous case (see Fig. 1). The AC-ARPES results in this case are dominated by an additional bright spot, P_N (circled) arising from scattering between the nodes. This vector can be also well

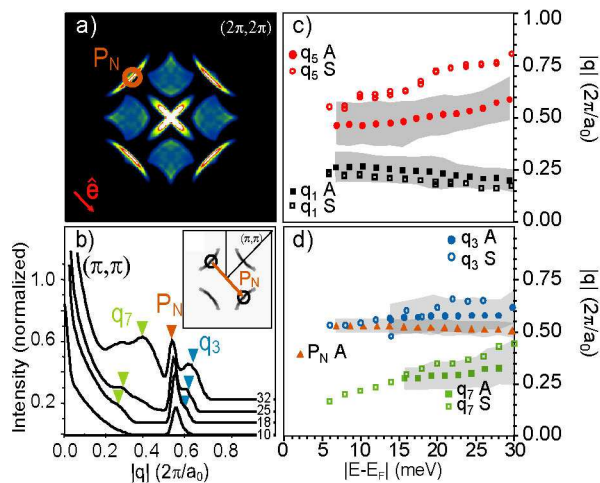


FIG. 4: a) AC-ARPES measured on the OPT92K crystal at -16 meV, in the triangle indicated, and with the photon polarization parallel to the ΓX direction (red arrow). One striking difference from Fig. 1 is the strong intensity along (π, π) . b) Normalized cuts along the (π, π) direction of the AC-ARPES intensity in a) (inset shows the origin of P_N and the octant in which the data was taken). Clearly the dominating feature is P_N . Small features can still be seen at the ‘octet’ wavevectors. c) ‘Octet’ wavevectors dispersions vs. energy along $\vec{q}||(\pi, 0)$. d) Dispersions of the ‘octet’ wavevectors and P_N feature along $\vec{q}||(\pi, \pi)$.

resolved above the gap energy, up to about 400 meV and disperses as the inverse of twice the nodal Fermi velocity as expected for node-node scattering. Cuts along the (π, π) direction are shown in panel b), where the P_N peak can be clearly observed, with respect to Fig. 3 c). The dispersion of this new scattering vector is plotted in panel d) and its location and dispersion makes it easy to identify it with the node-node scattering vector. The features associated with the ‘octet’ model are still evident in the AC-ARPES results for this photon polarization. Fig. 4 c) and d) show the dispersion of these \vec{q} -vectors as a function of energy below the gap value compared with the FT-STM results at the same doping. The agreement with FT-STM observed for this polarization is worse (see e.g. \vec{q}_5) than the one obtained in Fig. 3.

Based on these observations we propose that the better agreement between the AC-ARPES and the FT-STM for $\hat{e} \parallel \Gamma M$ compared to $\hat{e} \parallel \Gamma X$ is due to a suppression of nodal states in the STM spectra resulting from the tunneling matrix elements[15, 16]. In addition to explaining the vortex core results[16], this suppression strengthens JDOS features used to motivate the ‘octet’ model but without qualitatively changing their form. Simple theoretical JDOS calculations show that such a matrix element will indeed cause the flattening of the dispersion near zero-bias in the FT-STM data without the need for competing order parameters.[1, 3, 5, 8] While the energy resolution used here is still relevant for detailed discussion

of low energy states[8], the robust effect of the ARPES matrix element supports our proposal’s primacy.

In conclusion, the AC-ARPES analysis [10] was used to calculate the JDOS of $\text{Bi}_2\text{Sr}_2\text{CaCu}_2\text{O}_{8+\delta}$ for two different doping values, and the results were compared to FT-STM. The good agreement found between the two probes support the JDOS interpretation [6] used to explain the density of states modulation observed in FT-STM [1, 3]. In addition we have shown that by changing the photon polarization, and therefore the ARPES matrix element, we can gain new insights into the tunneling matrix element and its role in masking nodal states in STM experiments. This has implications concerning the vortex core spectra and the flattening of quasiparticle interference dispersions near E_F . Finally, AC-ARPES resolves weak features along $\vec{q}||(\pi, \pi)$ and outside the superconducting gap so far not reported by FT-STM.

We acknowledge and thank A. V. Balatsky, M. R. Norman, U. Chatterjee, A. Kaminskii for very helpful discussions and Mr. M. Ishikado for sample growth. This work was supported by the Director, Office of Science, Office of Basic Energy Sciences, Division of Materials Sciences and Engineering of the U.S Department of Energy under Contract No. DEAC03-76SF00098; by NSF Grant No. DMR03-49361 and DMR04-39768, and the Sloan Foundations.

* KPMcElroy@lbl.gov

- [1] J. E. Hoffman *et al.*, *Science* **297**, 1148 (2002).
- [2] C. Howald *et al.*, *Phys. Rev. B* **67**, 014533 (2003).
- [3] K. McElroy *et al.*, *Nature* **422**, 592 (2003).
- [4] K. McElroy *et al.* cond-mat/0404005.
- [5] K. McElroy *et al.*, *Phys. Rev. Lett.* **94**, 197005 (2005).
- [6] Q.-H. Wang and D.-H. Lee, *Phys. Rev. B* **67**, 020511(R) (2003).
- [7] L. Capriotti *et al.*, *Phys. Rev. B*, **68**, 014508 (2003).
- [8] S. Kivelson *et al.*, *Rev. Modern Phys.* **75**, 1201 (2003).
- [9] D. Podolsky *et al.*, *Phys. Rev. B* **67**, 094514 (2003).
- [10] R. S. Markiewicz, *Phys. Rev. B* **69**, 214517 (2004).
- [11] Ch. Renner *et al.*, *Phys. Rev. Lett.* **80**, 3606 (1998). S.H. Pan *et al.*, *Phys. Rev. Lett.* **85**, 1536 (2000).
- [12] Roland Wiesendanger, 1994, *Scanning Probe Microscopy and Spectroscopy*, (Cambridge University Press).
- [13] Hüfner, S., 1995, *Photoelectron Spectroscopy* (Springer, Berlin).
- [14] A similar line of inquiry has been taken by A. Kaminski and co-workers, to whom we are grateful for help; Utpal Chatterjee *et al* cond-mat/0505296.
- [15] I. Martin, *et al.*, *Phys. Rev. Lett.* **88**, 097003 (2002).
- [16] C. Wu, T. Xiang, and Z.B. Su, *Phys. Rev. B* **62**, 14427 (2000).
- [17] M. C. Asensio *et al.*, *Phys. Rev. B* **67**, 014519 (2003).
- [18] Backfolding in AC-ARPES was eliminated by setting the intensity to zero outside the first Brillouin zone to eliminate Umklapp processes absent in FT-STM.
- [19] A. Ghosal *et al.* cond-mat/0404005